LASER FLOW MEASUREMENTS OF SCATTERING AND FLUORESCENCE FROM CELL NUCLEI IN THE PRESENCE OF INCREASING Mg^{++} CONCENTRATIONS

M. GRATTAROLA,* P. CARLO,‡ G. GIANNETTI,* R. FINOLLO,‡ R. VIVIANI,* AND A. CHIABRERA*
*Biophysical and Electronic Engineering Department, University of Genoa, 16145 Genoa, Italy; and
‡Institute of Pharmacology, University of Genoa, 16132 Genoa, Italy

ABSTRACT The effects of Mg^{++} on the spatial organization of nuclei from rat hepatocytes are analyzed in the range 0–60 mM, in the presence of suitable concentrations of KCl to reproduce physiological conditions. It is shown that the scatter-signal distribution measured by means of a flow microfluorimeter is greatly affected by this range of Mg concentrations. By coupling this result to phase–contrast-automated image analysis, it is possible to identify a shrinking process induced by Mg^{++} in the range 0–2.5 mM, which reaches a plateau in the range 5–20 mM and is followed by a swelling process in the range 30–60 mM. The same Mg ranges are shown to affect the intercalation of the fluorochrome acridine orange into chromatin, suggesting that the shrinking-swelling phenomenon has also a molecular correspondence at the genome level. Possible implications in terms of the influence of Mg^{++} on the organization of chromatin inside intact cells are briefly discussed.

INTRODUCTION

Structural and functional information on chromatin can be obtained by perturbing the ionic composition of its surrounding medium. Ions can modulate chromatin condensation/dispersion, and this phenomenon is related to fundamental functional processes occurring in intact cells. When a quiescent cell, such as a frog erythrocyte or a human lymphocyte, is reactivated by an external trigger, an extremely complex sequence of biochemical events starts, leading to the synthesis of RNA, new proteins, and eventually DNA. Results in the literature suggest that these biochemical events are often preceded by an overall process of chromatin decondensation, leading to an increased accessibility of the cell genome. Among others, this process has been documented in nuclei of hen erythrocytes after cell fusion (Bolund et al., 1969), in nuclei of human lymphocytes after lectin stimulation (Darzynkiewicz et al., 1969), and in nuclei of frog erythrocytes after exposure to weak electromagnetic fields (Chiabrera et al., 1979). Coherently, an inverse process of chromatin condensation, related to decreased cellular activity, has been detected during the maturation process in spermatozoa (Gledhill and Campbell, 1973), and in cultured fibroblasts reaching confluence (Nicolini et al., 1977; Grattarola et al., 1981). All these observations suggest a link between cellular activity and chromatin structural organization.

On the other hand, several reports show that chromatin compactness can be dramatically affected by small variations in cation concentrations. Modifications to chromatin structure induced by alterations in the electrolyte medium have been studied in the past years, under various experimental conditions. At the nucleosome level, the morphology of chromatin and H1-depleted chromatin has been systematically studied by means of electron microscopy (Thoma et al., 1979). At the nuclear level, the condensation of whole nuclei as a function of ion concentration has been described by means of phase contrast microscopy (Olins and Olins, 1972). It has also been monitored (and correlated to RNA synthesis) by measuring the relative volumes of pellets (Hilder and Maclean, 1974) and by turbidity measurements on nuclear suspensions (Aaronson and Woo, 1981). In the work of Aaronson and Woo (1981), a possible involvement of the nuclear matrix in some of the above phenomena has also been suggested.

More or less, all the quoted methods exhibit some drawbacks. For example, a detailed morphological description is obtained by electron microscopy but the resulting picture may be difficult to extrapolate to the native state. On the other hand, turbidity and pellet measurements, as typical bulk measurements, give only average estimates of the parameters of interest. This drawback is particularly remarkable when the population of cells under investigation is not expected to be homogeneous, as in the case of the rat liver cells considered here. In fact, subpopulations with different levels of ploidity are usually present inside a population of hepatocytes (Pipkin et al., 1980; Deschenes et al., 1981); they can be affected by the ionic environment in different ways, and the variations in their relative proportions can modify, to some extent, the average value of the resulting signal.

In principle, phase-contrast microscopy seems to be a more useful technique but, besides the difficulty with

translating simple observations into quantitative structural data (Beltrame et al., 1984), it usually needs to be supported by other methods to improve the statistical significance of results. Here we show that the technique of laser-flow microfluorimetry, coupled to phase-contrast image analysis, can be used as a highly sensitive minimally perturbing method for monitoring ion-induced modifications of chromatin conformation in single intact nuclei, in the presence or absence of fluorescent intercalating probes.

Our results refer to modifications induced by the addition of small amounts of $MgCl_2$ to suspensions of nuclei already equilibrated with much larger amounts of KCl, to mimic the ionic composition of the cytoplasm. Liver cells have been selected in accordance with previous results in the literature that suggest that variations in chromatin compactness may occur after partial hepatectomy (Miller et al., 1979) and as an early effect induced by chemical carcinogens in vivo (Nicolini et al., 1982). Moreover, the isolation of nuclei from liver preparations shows a good reproducibility level. The main aim of our approach is to create physicochemical conditions that resemble, as closely as possible, the native physiological state of chromatin. Mg^{++} was chosen because the concentrations of Mg^{++} that have been proven to influence chromatin structure are comparable with the physiological values that are assumed to be present inside the nucleus (Hilder and McLean, 1974). Among the main cellular cations, this characteristic seems to be peculiar to Mg^{++}. In fact, it has not been verified conclusively for Ca^{++}, whose physiological concentrations seem to be in (or below) the micromolar range. On the other hand, both experimental evidence and theoretical calculations based on polyelectrolyte theory (Manning, 1978) show that monovalent cations are much less effective than divalent ones in affecting chromatin structure, so that greater (and unrealistic) variations in K^+ and Na^+ would be needed to cause the same effects on chromatin structure. Our goal is to identify the range of Mg^{++} concentrations that may control the spatial organization of chromatin inside a cell under physiological conditions. We think that the mildly perturbing methods described here should give a more realistic picture than other disruptive techniques of the in situ ionic balance responsible for the overall organization of nucleic material.

MATERIALS AND METHODS

Preparation of Cells and Nuclei

The experiments were mainly performed with nuclei obtained from rat liver cells. In a few cases, whole cells were also used. Sprague-Dawley male albino rats (50–60 *g* body weight, 3 wk old) that were starved for 18 h but allowed to drink a 7% sucrose solution were used in all the experiments. They were heparinized with 5 mg heparin/kg and anesthetized with 50 mg thiopental/kg, both injected intraperitoneally. Liver perfusion through the portal vein was carried out by injecting 70 ml of cold (4°C) Merchant's solution (0.14 M NaCl, 2.7 mM Na_2HPO_4, and 0.7 mM Na_2 EDTA, pH 7.5). The liver was excised and minced in 30 ml of cold dissociation medium (75 mM NaCl, 24 mM Na_2 EDTA, adjusted to pH 7.5 with NaOH). All subsequent steps were carried out at 4°C. The liver cell suspension was obtained by a loose-fitting homogenizer, and was filtered through a 200-mesh stainless steel sieve. Cells were collected from the filtrate by centrifuging for 3 min at 150 *g*. The pellet was resuspended in 4 vol of dissociation medium and 4 vol of water, which were added to hemolyze erythrocytes by osmotic shock. The suspension was centrifuged for 3 min at 150 *g*. The DNA, RNA, and protein ratios of the liver cells obtained by this standard protocol were ~1:0.35:19. Purified liver cell nuclei were prepared from the cell suspension as follows. The pellet was resuspended in 9 vol of solution consisting of 75 mM NaCl, 24 mM Na_2 EDTA, and 0.75% Triton X-100 (pH 7.5), and incubated for 4 min. The suspension was centrifuged for 3 min at 150 *g*, and this step was repeated once without further incubation. Finally, the pellet was washed once in 5 ml of dissociation medium. The average range of the weight ratios among the DNA, RNA, and proteins for these nuclei was ~1:0.09:3.3. According to previous work done on chromatin preparation (Nicolini et al., 1982*a*), these experimental conditions should induce minimal changes in chromatin structure inside the nuclei.

Laser Flow Microfluorimetry

Nuclei were suspended in a solution of KCl (mainly 150 mM KCl and, in a few cases, 120 and 170 mM KCl, as will be discussed in the Results). Cells were always suspended in 150 mM NaCl. All the biological samples were analyzed by means of a FACS III (Becton Dickinson, Mountain View, CA) cell sorter (Bonner et al., 1972), setting the laser exciting wavelength to 488 nm. In this system, a laminar flow of the particles under study is generated. The particles are forced to pass, one at a time, in front of a laser beam at the rate of up to 10^3/s. As a result of this interaction, the light is partially transmitted, diffracted, and reflected. A detector, aligned with the laser beam and the interacting object, collects the forward light scatter, while an obscuration bar prevents the collection of the direct beam, so that only the light scattered at narrow angles (1–15°) is collected.

At a 90° angle to the laser beam, there are other detectors, that are routinely used for fluorescence measurements, which are performed by staining biological samples with a fluorochrome. At the beginning of each experiment the microfluorimeter was calibrated by means of fluorescent beads 4.43 μm in diam, SD 0.31 (Polysciences, Inc., Warrington, PA). The system was considered ready for the biological samples when scatter and fluorescence histograms, obtained by running the beads, reached coefficients of variation <10 and 12%, respectively. At the end of each experiment the performance of the system was checked using the same beads; the dispersion range turned out to be the same for each experiment. In the present work, the system was used in two different configurations.

Scattering Measurements Only. In this configuration, the signal from unstained samples was collected, mainly by means of the forward detector and, in a few cases, by means of one of the two 90° detectors, in front of which neutral density filters had been interposed.

Scattering and Fluorescence Measurements. In this configuration, light scattered in the forward direction was collected, and fluorescent light from stained cells and nuclei was collected by the two 90° detectors, in front of which optical filters had been interposed for cutting off the exciting light and selecting the appropriate emission band. For this second set of experiments, the fluorescent dye acridine orange (AO) was used as a probe for the DNA amount and the overall chromatin accessibility. The dye is known to intercalate (as a cation) in monomeric form between the DNA base pairs, while the experimental conditions used ($2 \cdot 10^{-5}$ M final AO concentration and $3 \cdot 10^5$ nuclei/ml) should guarantee the absence of undesired secondary processes (e.g., stacking) (Nicolini et al., 1979; Beltrame et al., 1981). Because the intercalation process results in the emission of green fluorescent light, whereas the stacking process induces a shift to longer wavelengths (orange-red), a

qualitative control of the staining procedure can be easily performed by visual inspection with a fluorescence microscope; our experimental conditions were periodically checked in this way. Moreover, the intensity of the green fluorescence emission was monitored with the flow system by measuring the position of the peak channel of the fluorescence distribution, as a function of increasing AO concentration. This saturation curve was repeated several times, always giving approximately the maximum intensity value of the green emission under the given staining conditions.

Phase Contrast Image Analysis

Some of the unstained nuclei analyzed with the flow microfluorimeter were also observed by means of phase-contrast microscopy. A general-purpose image analyzer developed in our laboratory (ACTA [Automated Cell Texture Analyzer] system; see Beltrame et al., 1980) was used.

The system includes a microscope for fluorescence measurements, connected with an intensified ISIT TV camera (RCA, Lancaster, PA) and a microscope for absorption and phase contrast measurements, connected with a Plumbicon TV camera (Bosch, Darmstadt, Federal Republic of Germany), which was used for the described experiments.

In the ACTA system, the video signal is sent to a fast analog-to-digital converter, which digitalizes the signal in real time, according to a format of 512 × 512 picture points per frame, with 8-bit resolution in light intensity (i.e., 256 gray levels) for each picture point. The digitalized image is stored in real time in a buffer memory (VDC501; Tesak, Florence, Italy). In this way it is possible to freeze any video frame coming out from one of the two TV scanners. Inside the buffer memory there are programmable look-up tables, which allow one to perform transformations in real time on the memory content (pseudocolor, etc.). The buffer memory is interfaced with an HP1000 minicomputer (Hewlett Packard Co., Palo Alto, CA), which controls the transfer of the image to a mass-memory device (disk cartridge or magnetic tape) and allows further elaborations of the stored images. The original images and the elaborated ones can be visualized by means of a color monitor where any arbitrary range of gray levels of the image can be identified by associating a color with it (pseudocolor) by means of appropriate look-up tables.

The images are software equalized off line for uneven illumination and nonuniformity of the TV target by using blank images (black and white), previously stored during the acquisition process. Software routines allow the measurements of densitometric parameters (e.g., integrated optical densities), geometric parameters (e.g., areas) and derived ones (e.g., average optical densities). The measurements are made on subregions of the image selected by means of programmable electronic windows and by considering only any selected range of gray levels.

For the purposes of the present results, only the area (A) of the phase contrast image of each nucleus (that is, the total number of picture points belonging to each individual nuclear image) was measured. A 40 × phase contrast objective (Phaco 2; Leitz, Federal Republic of Germany) was used for the measurements. The overall measurement SD was ~1%.

RESULTS

Acridine Orange Microfluorimetry of Intact Nuclei and Cells

Measurements of the fluorescence intensity resulting from the intercalation of dyes between the DNA base pairs are frequently performed to obtain information about DNA accessibility in chromatin under various physiological conditions. This approach is quite a sensitive one, even if the control of all the staining steps is rather difficult (Nicolini et al., 1979; Beltrame et al., 1981).

We attempted to measure the Mg^{++}-induced modifications to chromatin structure and to relate them to chromatin organization inside a cell. Toward this end, we analyzed the availability of chromatin to AO intercalation as a function of Mg^{++} concentrations, and we compared it with its availability in intact cells. The results are summarized in Fig. 1. The left panel shows the peak position of the fluorescence histogram (green emission) of stained nuclei vs. the concentration of added $MgCl_2$, in the presence of 150 mM KCl. In the right panel, the peak position of the fluorescence histogram of AO stained nuclei (in the presence of 120, 150, and 170 mM KCl, respectively) is normalized to the peak position of the fluorescence histogram of AO stained intact cells (150 mM NaCl). The data are plotted vs. increasing Mg^{++} concentrations. This panel is intended to be a preliminary comparison between the ionic conditions of an isolated nucleus and the ionic environment experienced by a nucleus inside a cell. The data suggest that, considering the presence of mitochondrial DNA and of double-stranded RNA inside the cyto-

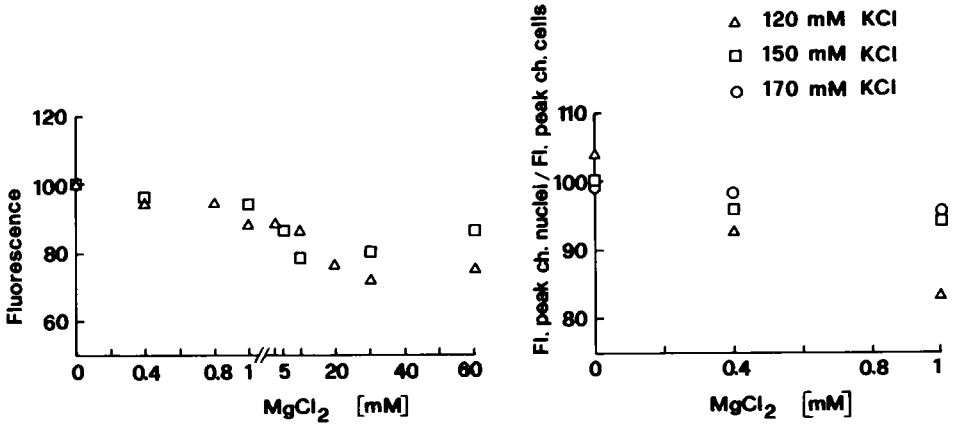

FIGURE 1 *Left*: peak position (chromatin accessibility) of the fluorescence distribution of AO-stained nuclei (in the presence of 150 mM KCl; two sets of experiments) normalized to the peak of the histogram obtained in the absence of Mg^{++}. *Right*: peak position of the fluorescence distribution of AO-stained nuclei, indicated as Fl. peak ch. nuclei, normalized to the peak position of the fluorescence distribution of AO-stained cells, indicated as Fl. peak ch. cells, (150 mM NaCl). On the *right* different symbols denote different KCl concentrations in the suspending medium.

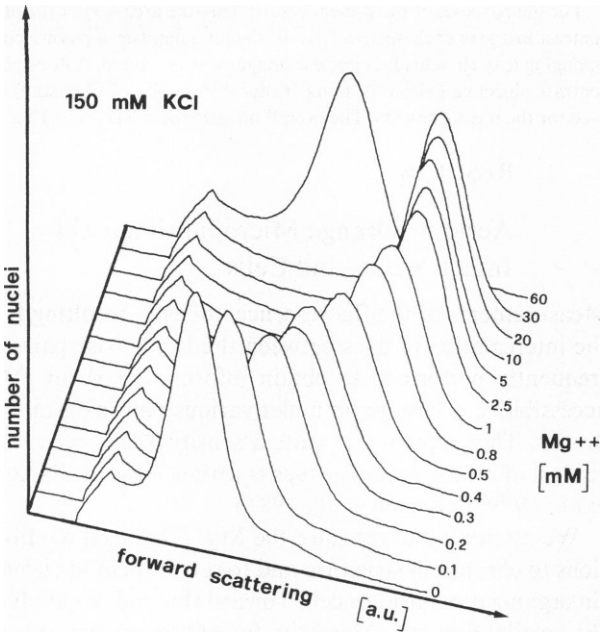

FIGURE 2 Forward light-scattering histograms of rat hepatocytes' nuclei as a function of Mg^{++} are shown. All histograms originate from the collection of 3×10^4 events and are normalized to 100 for display purposes.

plasm, values of KCl concentrations near 150 mM can be used as a starting point for the simulation of ionic media sufficiently close to the native one.

Forward Light-Scattering Measurements on Unstained Nuclei

According to the results described in the previous section, the spatial organization of nuclei in the presence of KCl in the range 120–170 mM is somehow comparable to their organization inside intact cells, at least with respect to microfluorimetric measurements. Since we had no compelling reasons for selecting a specific KCl concentration in the above quoted range, we decided to explore the effects on chromatin of Mg^{++} in the presence of 150 mM KCl. Under these experimental conditions, the effects on the forward light-scatter signal caused by addition of $MgCl_2$, in the range from 0 to 60 mM, are those shown in Fig. 2. The figure summarizes a typical experimental result where the actual shape of each signal distribution resulting from the forward light scattering is plotted as a function of increasing Mg^{++} concentrations. Each histogram represents $3 \cdot 10^4$ events distributed over 256 channels, and it is the smoothed version (i.e., the average on a 10-by-10-point scale) of the real histogram, which is previously sent from the multichannel analyzer of the microfluorimeter to the magnetic tape unit of a minicomputer (HP 1000; Hewlett Packard Co.). The first (left) peak of each histogram is mainly due to fragments of nuclei and membranes. The second peak refers to the main distribution of the nuclei population. Usually, a smaller third peak can be observed, resulting from nuclei with larger DNA amounts. This peak is not shown in the figure because it falls out of the scale in Fig. 2. This kind of analysis was repeated several times and the final results are summarized in Fig. 3, where each data point refers to the channel of the distribution peak of the analyzed population, normalized to the peak position in the absence of Mg^{++}. Each point is the average, over six experiments, of Mg^{++} concentrations in the range 0.1–0.3 mM (0.1 mM, 0.2 mM, and 0.3 mM), whereas the other points are the averages, over five experiments, of Mg^{++} concentrations in the range 0.4–60 mM (0.4, 0.5, 0.8, 1,

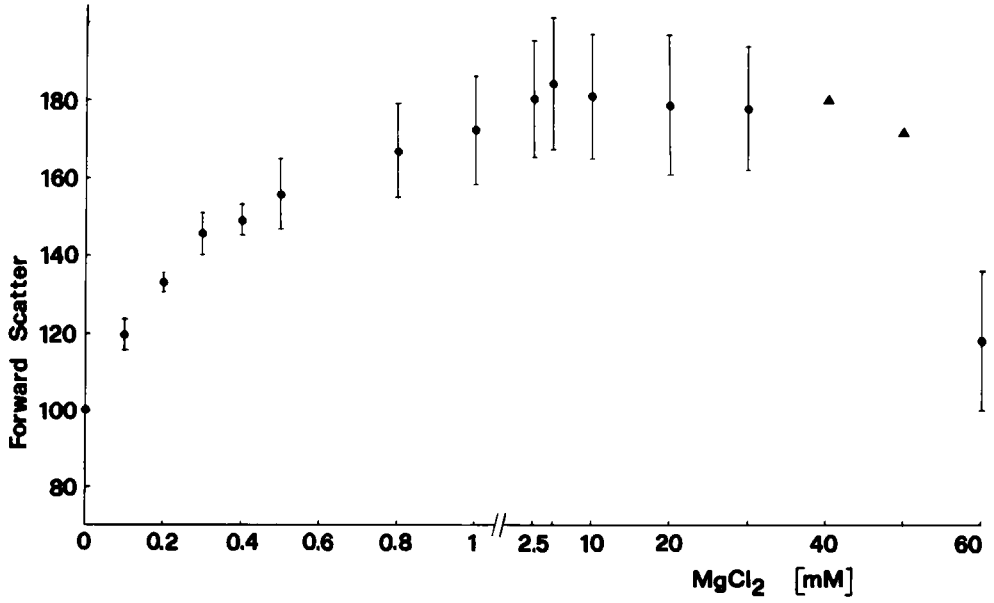

FIGURE 3 The channel of the peak of each experimental histogram is normalized to the histogram obtained in the absence of Mg^{++} and plotted as a function of $MgCl_2$. Bars denote SD. ▲ indicates single experiments.

2.5, 5, 10, 20, and 60 mM), except for 40 and 50 mM concentrations, which are single measurements. Bars represent SD for each point. A few experiments were also performed starting with 120 and 170 mM KCl solutions, respectively. They showed a trend that was in qualitative agreement with the results in Fig. 3 (data not shown).

A few tests of the reversibility of the observed phenomena were also performed. Nuclei equilibrated in 2.5 mM $MgCl_2$ were diluted 10 times in 150 mM KCl. The recorded scattering signal fell well inside the range of values measured for nuclei equilibrated in 0.2–0.3 mM $MgCl_2$. Interestingly enough, the scatter signal from nuclei equilibrated in 60 mM $MgCl_2$, and diluted ~20 times (in 150 mM KCl) remained substantially lower than the average signal produced by nuclei in the presence of 2.5 mM $MgCl_2$. The variation in the signal reached only ~40% of the value that should be expected in the case of a full reversibility.

Fig. 4 depicts, with the same format as in Fig. 2, a distribution of histograms resulting from the acquisition of the 90° light scattering, according to the procedure described in the Methods section. This measurement was repeated three times with comparable results, but no statistical analysis of the data is presented. By comparing Fig. 2 with Fig. 4, it can be observed that, whereas in the case of the forward light scattering the $MgCl_2$-induced effects on chromatin result mainly in a shift in the peak position, with slight changes in the variance of each histogram, for the 90° light scattering the situation is almost the opposite, the main effect being a modulation in the broadening of each distribution. See Discussion for an interpretation.

Phase-Contrast Measurements on Unstained Nuclei

During one of the experiments reported, a drop from each of seven tubes of suspensions of nuclei (in the presence of 0, 0.3, 0.8, 1, 2.5, 30, and 60 mM, respectively) was placed on a slide. Each slide was covered with a coverslip and immediately inspected by means of the ACTA system under phase-contrast conditions. Five nuclei for each slide were randomly selected and their digitalized images were stored on magnetic tape, according to the procedure described in the Methods section. The images were then analyzed off-line, and for each of them, the number of picture points belonging to each nucleus was measured. To measure each nuclear image as a distinct entity as compared with the background, we chose an appropriate band of gray levels that selectively identified the nuclei against the background. The results of these measurements are given in Fig. 5 and a collage of images (one for each experimental condition) is shown in Fig. 6. In the presence of 60 mM $MgCl_2$, the nuclei appear to be swollen as compared with the control images (in both types of images, some nucleoli are easily detectable), whereas, in the other

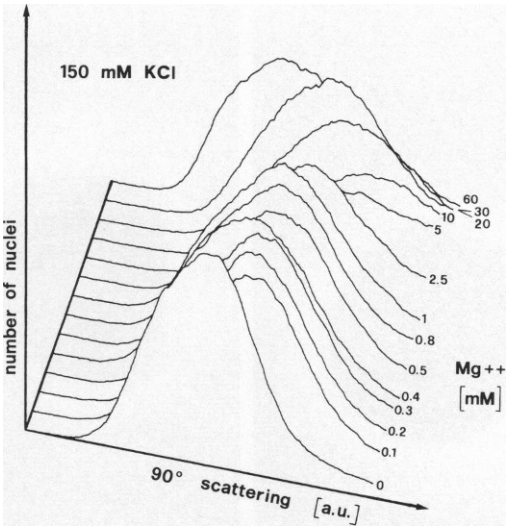

FIGURE 4 Wide-angle scattering histograms of rat hepatocytes nuclei as a function of Mg^{++} are shown. The detector is at 90° to the laser beam. The format is the same as in Fig. 2.

cases the nuclei have obviously shrunk, especially in the presence of 2.5 and 30 mM Mg^{++}. The easy identification of some nucleoli in the control images (and also in the presence of 0.3 mM $MgCl_2$) is further proof of the good preservation of the nuclear structures in the presence of 150 mM KCl and small amounts of $MgCl_2$. This observation can be evidenced by comparison with images of intact cells (not shown).

DISCUSSION

Measurements on Unstained Nuclei: Morphological Considerations

The main results obtained with the flow microfluorimeter are those of Fig. 3. The scattering signal increases as a function of Mg^{++} concentrations up to ~2.5 mM. Then it becomes virtually insensitive to variations in Mg^{++} concen-

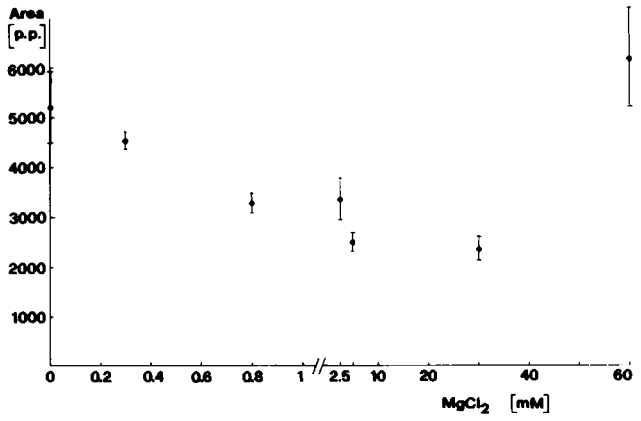

FIGURE 5 The area (in picture points) of the phase-contrast images of nuclei, plotted as a function of $MgCl_2$ is shown. Bars denote SD.

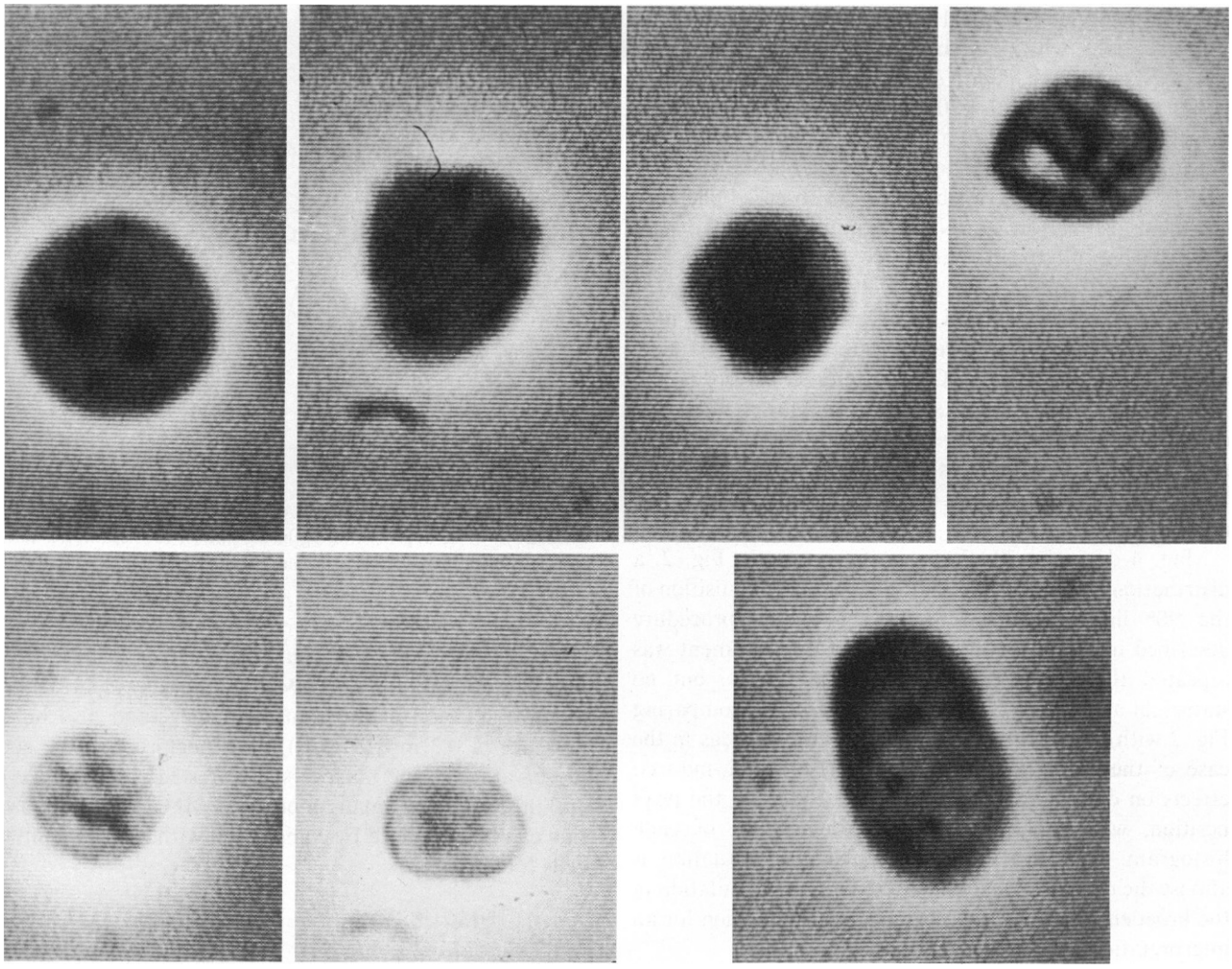

FIGURE 6 The collage of phase-contrast images of nuclei, taken directly from one of the ACTA system displays is shown. From the *top left* corner to the *bottom right* corner: 0 mM $MgCl_2$, 0.3 mM $MgCl_2$, 0.8 mM $MgCl_2$, 1 mM $MgCl_2$, 2.5 mM $MgCl_2$, 30 mM $MgCl_2$, and 60 mM $MgCl_2$.

trations in the approximate range 5–30 mM, and finally it decreases, dropping down to values comparable to those in the absence of Mg^{++}, for 60 mM Mg^{++}. A more speculative interpretation of the data would suggest a two-step initial variation, with a steeper increase in the signal for $MgCl_2$ values up to 0.3 mM and a less steep increase for Mg^{++} values up to 2.5 mM Mg^{++}.

The coupling of these results to the phase-contrast images allows us to associate the increase in the scattering signal with the shrinking of the nuclear components and the decrease in the signal with their swelling. This interpretation deserves further comments before discussing its biological relevance. In fact, it is often stated that the forward scatter signal recorded by a flow microfluorimeter is somehow proportional to the size of the scattering object. This is approximately true for smooth spherical objects where size is the only variable. Obviously, our case is much more complex, and it is possible to associate at least three different phenomena with the shrinking process, namely, a decrease in the global volume, local variations in the refractive index (due to changes in macromolecular concentrations), and an increase in the surface roughness. To correctly model the interplay between these phenomena, much more complex objects than a sphere are needed, and approaches using coated spheres (Meyer and Brunsting, 1975) should be combined with studies of random distributions of transparent hard spheres (Bettelheim and Siew, 1983).

It will suffice here to recall that, as reported in the literature, in the case of human erythrocytes, a decrease in the cell diameter coupled with the formation of spicules results in an increase in the forward-scattering signal (Eisert, 1979). The behavior of the 90° light-scatter histograms can also be interpreted in the light of a shrinking process. More precisely, the indication that an increase in Mg^{++} concentrations is paralleled by a broadening of the signal distribution can be considered further proof of an increase in the internal structure of an object due to a

shrinking process. In fact, at large angles (≥90°), the scatter signal is known to be much more sensitive to the object's internal structure than to its volume (Kerker et al., 1978) so that the broadening of the signal distribution can be related to the many ways in which highly structured, randomly oriented objects can be intercepted by a laser beam.

An obvious interpretation of the data so far discussed is that variations in Mg^{++} concentrations can directly affect chromatin structure. As already pointed out in the Introduction, a cation-induced transition in chromatin at different levels has been observed by many authors, including the 10 nm → 30 nm transition of chromatin fibers (Thoma et al., 1979), chromatin precipitation induced by a high concentration of Na^{+} (Fulmer and Bloomfield, 1981), and the compaction of histone-depleted nuclei (Lebkowski and Laemmli, 1982) in the presence of divalent cations. According to polyelectrolyte theory (Manning, 1978), a condensation phenomenon could be due to a decrease in the electrostatic repulsive forces originated by the negative charges of DNA, that can be neutralized by addition of Mg^{++}. On the other hand, for higher values of added cation, a swelling phenomenon can be easily justified by assuming that the onset of a process that removes histones and other proteins from chromatin structure. The removal hypothesis is corroborated by the experiments performed by recording the scatter signal from nuclei initially equilibrated in the presence of 60 mM Mg^{++} and then shifted to 2.5 mM Mg^{++}. In fact, as already noted, the signal does not go back to the usual value displayed in the presence of 2.5 mM Mg^{++}, suggesting the onset of irreversible phenomena.

A different interpretation of the data, namely, an indirect action of Mg^{++} on chromatin, mediated by effects induced by the so-called "nuclear matrix," cannot be excluded, especially for the shrinking process. In fact, it is generally accepted that chromatin is attached to a framework inside the interphase nucleus, and an interaction of DNA with the nuclear matrix has been proposed as a cause for DNA compaction in the case of histone-depleted nuclei in the presence of divalent cations (Lebkowski and Laemmli, 1982). On the other hand, a direct action of Mg^{++} on chromatin is somehow suggested by a few results (not shown) that indicate that, in the absence of Mg^{++}, AO alone, which is known mainly to intercalate DNA, can affect the forward-scattering signal to some extent and in the same direction as Mg^{++}. Finally, our present results do not exclude the possible involvement of RNA, which has been proposed to be involved in the maintenance of interphase chromosome structure (Benyajati and Worcel, 1976).

On the basis of the trend of the scatter signal and of the images obtained by phase-contrast microscopy, it is easy to speculate that Mg^{++}, in four different ranges, can affect (directly or indirectly) chromatin organization in rat hepatocyte nuclei in various ways. For large (i.e., >30 mM) concentration values, nuclei become swollen and chromatin become dispersed. In the range of 30–5 mM, gross effects in (reduced) nuclear volumes are not evident, and only a different local organization of the nuclear material can be assumed, possibly with the appearance of discrete structures but without any obvious trend. To preserve a high level of chromatin condensation, it seems necessary to maintain Mg^{++} in the range 2.5–0.4 mM. Finally, below 0.4 mM Mg^{++}, chromatin relaxes quite abruptly to the value measured in the absence of Mg^{++}.

Measurements on Stained Nuclei and Cells: Functional Considerations

The process of AO intercalation can be considered a simulation of the accessibility of the genome to biological molecules under physiological conditions. As already indicated in the literature (Traganos et al., 1976; Beltrame et al., 1981), changes in Mg^{++} concentrations can affect the intercalation process by modifying the number of available binding sites (while interfering with the stacking process by modifying its equilibrium constant). A decrease in the fluorescence intensity (green emission-intercalation process) can be assumed, as a first approximation, to indicate a reduction in the availability of binding sites. From this point of view, the results of the first panel in Fig. 1 clearly show that the intercalation process decreases during the shrinking process and increases during the swelling process. Then, it can be concluded that the gross phenomenon measured by the scattering signal and observed by phase-contrast microscopy is the manifestation of events occurring at the molecular level, meaning that a different exposure of DNA to external agents in intact nuclei can be obtained by controlling Mg^{++} concentrations over a narrow range. This observation is in accordance with previous results (Hilder and Maclean, 1974), which show different rates of RNA synthesis in intact nuclei of erythrocytes as a function of the ionic strength. Obviously, to associate any physiological meaning with this observation, we must prove that this phenomenon can also be induced in intact cells, and that the same Mg^{++} ranges, as identified by our experiments, are present inside a nucleus surrounded by its natural cellular structures, where such ranges determine, to some extent, cellular activity. The results of the right part of Fig. 1 suggest that the intercalation process in isolated nuclei in the presence of 120–170 mM KCl and 0–1 mM $MgCl_2$ can be compared with the intercalation process in nuclei inside intact cells. Then, in principle, the accessibility of the genome in the two cases is comparable, irrespective of the variables introduced by other sources of intercalation present inside the cytoplasm, like double-stranded RNA and mitochondrial DNA.

Clearly, much more work needs to be done to gain a deeper understanding of the functional relevance of Mg^{++} inside a cell nucleus under physiological conditions. Nevertheless, it is tempting to associate a physiological mean-

ing with the range of Mg^{++} concentrations required to start (0.4–2.5 mM) a condensed chromatin state. From this point of view, we identify such a range as a sort of physiological threshold that separates states that are metabolically more active from more quiescent ones. A cell could jump from one state to another as a consequence of a sudden modification in chromatin compactness induced by a small but critical variation in Mg^{++} concentration inside the nucleus.

This work was supported in part by the Consiglio Nazionale delle Ricerche (CNR) of Italy and in part by Special Project "Control of Neoplastic Growth" (CNR), grant #83.00742.96. One of the authors (M. G.) was also supported by a grant from the Ministero della Pubblica Istrutione.

Received for publication 2 May 1984 and in final form 23 August 1984.

REFERENCES

Aaronson, R., and E. Woo. 1981. Organization in the cell nucleus: divalent cations modulate the distribution of condensed and diffuse chromatin. *J. Cell Biol.* 90:181–186.

Beltrame, F., A. Chiabrera, M. Grattarola, P. Guerrini, G. Parodi, D. Ponta, G. Vernazza, and R. Viviani. 1980. ACTA: Automated image analysis system for absorption, fluorescence, and phase contrast studies of cell images. *IEEE Proc. Annu. Conf. Engin. Med. Biol. Soc. 2nd* 58–60.

Beltrame, F., A. Chiabrera, M. Grattarola, P. Guerrini, G. Parodi, D. Ponta, G. Vernazza, and R. Viviani. 1981. Re-evaluation of acridine orange stain for flow cytometry. *Bioelectrochem. Bioenerg.* 8:387–404.

Beltrame, F., B. Bianco, and A. Chiabrera. 1984. Automated analysis of living cells through the quantitative use of automated phase contrast microscopy. *Cell Biophys.* 6:103–116.

Benyajati, C., and A. Worcel. 1976. Isolation, characterization, and structure of folded interphase genome of Drosophila melanogaster. *Cell.* 9:393–407.

Bettelheim, F. A., and E. L. Siew. 1983. Effect of change in concentration upon lenses turbidity as predicted by the random fluctuations theory. *Biophys. J.* 41:29–33.

Bolund, L., N. Ringertz, and H. Harris. 1969. Changes in the cytochemical properties of erythrocytes nuclei reactivated by cell fusion. *J. Cell Sci.* 4:71–87.

Bonner, W., H. Hulett, R. Sweet, and L. Herzenberg. 1972. Fluorescence activated cell sorting. *Rev. Sci. Instrum.* 43:404–420.

Chiabrera, A., M. Hinsenkamp, A. A. Pilla, J. Ryaby, D. Ponta, A. Belmont, F. Beltrame, M. Grattarola, and C. Nicolini. 1979. Cytofluorometry of electromagnetically controlled cell dedifferentiation. *J. Histochem. Cytochem.* 27:375–381.

Darzynkiewicz, Z., L. Bolund, and N. Ringertz. 1969. Actinomycin binding of normal and phytohaemagglutinin stimulated lymphocytes. *Exp. Cell Res.* 55:120–132.

Deschenes, J., J. P. Valet, and N. Marceau. 1981. The relationship between cell volume, ploidity, and functional activity in differentiating hepatocytes. *Cell Biophys.* 3:321–334.

Eisert, W. G. 1979. Cell differentiation based on absorption and scattering *J. Histochem. Cytochem.* 27:404–409.

Fulmer, A. W., and V. A. Bloomfield. 1981. Chicken erythrocyte nucleus contains two classes of chromatin that differ in micrococcal nuclease susceptibility and solubility at physiological ionic strength. *Proc. Natl. Acad. Sci. USA.* 78:5968–5972.

Gledhill, B. L., and G. L. M. Campbell. 1973. Microfluorimetric comparison of chromatin during cytodifferentiation. *In* Fluorescence Techniques in Cell Biology. A. A. Thaer and M. Servetz, editors. Springer-Verlag, New York. 151–162.

Grattarola, M., A. Belmont, and C. Nicolini. 1981. Correlation between Barr body and overall chromatin decondensation" in vitro." *J. Cell Sci.* 47:187–195.

Hilder, V. A., and N. Maclean. 1974. Studies on the template activity of isolated *Xenopus* erythrocyte nuclei. I. The effects of ions. *J. Cell Sci.* 16:133–142.

Kerker, M., D. Cooke, H. Chew, and P. McNulty. 1978. Light scattering by structured spheres. *J. Opt. Soc. Am.* 592–601.

Lebkowski, J. S., and U. K. Laemmli. 1982. Evidence for two levels of DNA folding in histone-depleted HeLa interphase nuclei. *J. Mol. Biol.* 156:309–324.

Manning, G. 1978. The molecular theory of polyelectrolyte solutions with applications to the electrostatic properties of polynucleotides. *Quart. Rev. Biophys.* 11:179–246.

Miller, P., W. A. Linden, and C. Nicolini. 1979. Physico-chemical studies of isolated chromatin compared with "in situ" chromatin after partial hepatectomy in the rat. *Z. Naturforsch. Sect. C. Biosci.* 34c:442–448.

Meyer, R. A., and A. Brunsting. 1975. Light scattering from nucleated biological cells. *Biophys. J.* 15:191–203.

Nicolini, C., W. Giaretti, C. DeSaive, and F. K. Kendall. 1977. The G0-G1 transition of WI38 cells. *Exp. Cell Res.* 106:119–125.

Nicolini, C., A. Belmont, S. Parodi, S. Lessin, and S. Abraham. 1979. Mass action and acridine orange staining: static and flow cytofluorometry. *J. Histochem. Cytochem.* 27:102–113.

Nicolini, C., P. Carlo, A. Martelli, R. Finollo, F. A. Bignone, E. Patrone, U. Trefiletti, and G. Brambilla. 1982*a*. Viscoelastic properties of native DNA from intact nuclei of mammalian cells. *J. Mol. Biol.* 161:155–175.

Nicolini, C., A. Martelli, M. Grattarola, G. Starace, and R. Viviani. 1982*b*. Early effects of chemical carcinogens as compared to induced cell proliferation. I. Flow microfluorimetry. *Basic Appl. Histochem.* 26:143–152.

Olins, D. E., and A. L. Olins. 1972. Physical studies of isolated eukaryotic nuclei. *J. Cell Biol.* 53:715–736.

Pipkin, J. L., W. G. Hinson, J. L. Hudson, J. L. Martin, B. M. North, and L. D. Pack. 1980. The effect of isoproterenol on nuclear protein synthesis in electrostatically sorted rat hepatocytes. *Cytometry.* 1:212–221.

Thoma, F., T. Koller, and A. Klug. 1979. Involvement of histone H1 in the organization of the nucleosome and of the salt-dependent superstructures of chromatin. *J. Cell Biol.* 83:403–426.

Traganos, F., Z. Darzynkiewicz, T. Sharpless, and M. R. Melamed. 1976. Cytofluorometric studies on conformation of nucleic acids in situ. I. Restriction of acridine orange binding by chromatin proteins. *J. Histochem. Cytochem.* 24:40–48.